Isolobal Zwitterionic Niobium and Tantalum Imido and Zirconium Monocyclopentadienyl Complexes: Theoretical and Methyl Methacrylate Polymerization Studies

Rocío Arteaga-Müller,[†] Javier Sánchez-Nieves,[†] Javier Ramos,[‡] Pascual Royo,*[,†] and Marta E. G. Mosquera[†,§]

Departamento de Química Inorgánica, Universidad de Alcalá, Campus Universitario, E-28871 Alcalá de Henares, Madrid, Spain, and Grupo de Estructura Molecular y Propiedades de Polimeros, Instituto de Estructura de la Materia, CSIC, Serrano 113bis, 28006, Madrid, Spain

Received October 24, 2007

The trichloro derivatives $[MCl_3(NR)(py)_2]$ reacted with LiOAr to give the imido aryloxo complexes $[MCl_2(NR)(OAr)(py)_2]$ (M = Nb, R = *t*Bu (**1a**), Ar (**1b**); M = Ta, R = *t*Bu (**2a**); Ar = 2,6-*i*Pr$_2$C$_6$H$_3$) and were alkylated with [BzMgCl], affording the tribenzyl derivatives $[NbBz_3(NR)]$ (R = *t*Bu (**3a**), Ar (**3b**)). Similar alkylations of the aryloxo derivatives **1** and **2** gave the dibenzyl complexes $[MBz_2(NR)(OAr)(THF)]$ (M = Nb, R = *t*Bu (**5a**); M = Ta, R = *t*Bu (**6a**), Ar (**6b**)). The zwitterionic imido complexes $[MBz_2(NtBu)\{\eta^6\text{-}C_6H_5CH_2E(C_6F_5)_3\}]$ (M = Nb, E = B (**7a-B**), Al (**7a-Al**); M = Ta, E = Al (**8a-Al**)) were obtained upon addition of 1 equiv of $E(C_6F_5)_3$ (E = B, Al) to the tribenzyl derivatives $[MBz_3(NtBu)]$ (M = Nb (**3a**), Ta (**4a**)). The aryloxo compound **6a** reacted with 2 equiv of the Lewis acids $E(C_6F_5)_3$ (E = B, Al) to give the corresponding zwitterionic imido complexes $[TaBz(NtBu)(OAr)\{\eta^6\text{-}C_6H_5CH_2E(C_6F_5)_3\}]$ (E = B (**11a-B**), Al (**11a-Al**)) and the adduct (THF)·$E(C_6F_5)_3$, through two different intermediates, the ionic $[TaBz(NtBu)(OAr)(THF)][BzB(C_6F_5)_3]$ (**9a**) for E = B and the neutral $[TaBz_2(NtBu)(OAr)]$ (**10a**) for E = Al. The related monocyclopentadienyl complex $[ZrCpBz_2\{\eta^6\text{-}C_6H_5CH_2Al(C_6F_5)_3\}]$ (**12-Al**) was also isolated by reaction of $[ZrCpBz_3]$ with $Al(C_6F_5)_3$. DFT calculations were carried out to further understand this type of zwitterionic imido derivative in comparison with the isolobal zirconium cyclopentadienyl compound $[ZrCpBz_2\{\eta^6\text{-}C_6H_5CH_2B(C_6F_5)_3\}]$. MMA polymerization was investigated for the $[MBz_2X(NtBu)]/E(C_6F_5)_3$ (X = Bz, OAr) and $[ZrCpBz_3]/E(C_6F_5)_3$ (E = B, Al) systems.

Introduction

The imido group is a strong π donor ligand with the widely proven ability to stabilize high-valent metal complexes.[1,2] The isolobal relationship of the imido and the cyclopentadienyl ligands[3] is an important feature that allows the half-sandwich imido complexes $[MCp(NR)X_2]$ (M = group 5 metal) to be studied as isoelectronic counterparts of dicyclopentadienyl derivatives $[MCp_2X_2]$ (M = group 4 metal).[3–16] The reactivities of these two types of complexes are comparable, although the half-sandwich complexes $[MCp(NR)X_2]$ (M = group 5 metal) were rather less active olefin polymerization catalysts than the metallocene-type complexes $[MCp_2X_2]$ (M = group 4 metal).[17–19] This difference has been attributed to the lower acidity of group 5 metal derivatives, which would consequently be expected to show a greater affinity for polar olefins. Conversely, important differences between these two types of complexes involve the reactivity of the metal−nitrogen multiple bond.[13,20–23]

Control of the stereochemistry and polydispersity of the polymer chain and the production of well-defined block

* To whom correspondence should be addressed. E-mail: pascual.royo@uah.es; FAX: 00 34 91 885 4683.
[†] Universidad de Alcalá.
[‡] Instituto de Estructura de la Materia, CSIC.
[§] X-ray diffraction studies.

(1) Nugent, W. A.; Mayer, J. M. *Metal Ligand Multiple Bonds*; Wiley-Interscience: New York, 1988.
(2) Wigley, D. E. *Prog. Inorg. Chem.* **1994**, *42*, 239.
(3) Williams, D. N.; Mitchell, J. P.; Poole, A. D.; Siemeling, U.; Clegg, W.; Hockless, D. C. R.; O'Neil, P. A.; Gibson, V. C. *J. Chem. Soc., Dalton Trans.* **1992**, 739.
(4) Chan, M. C. W.; Cole, J. M.; Gibson, V. C.; Howard, J. A. K.; Lehmann, C.; Poole, A. D.; Siemeling, U. *J. Chem. Soc., Dalton Trans.* **1998**, 103.
(5) Gibson, V. C.; Poole, A. D. *J. Chem. Soc., Chem. Commun.* **1995**, 2261.
(6) Gibson, V. C.; Poole, A. D.; Siemeling, U.; Williams, D. N.; Clegg, W.; Hockless, D. C. R. *J. Organomet. Chem.* **1993**, *462*, C12.
(7) Cockcroft, J. K.; Gibson, V. C.; Howard, J. A. K.; Poole, A. D.; Siemeling, U.; Wilson, C. *J. Chem. Soc., Chem. Commun.* **1992**, 1668.
(8) Poole, A. D.; Gibson, V. C.; Clegg, W. *J. Chem. Soc., Chem. Commun.* **1992**, 237.
(9) Postigo, L.; Sánchez-Nieves, J.; Royo, P. *Inorg. Chim. Acta* **2007**, *360*, 1305.
(10) Arteaga-Müller, R.; Sánchez-Nieves, J.; Royo, P.; Mosquera, M. E. G. *Polyhedron* **2005**, *24*, 1274.
(11) Sánchez-Nieves, J.; Royo, P. *J. Organomet. Chem.* **2001**, *621*, 299.
(12) Sánchez-Nieves, J.; Royo, P.; Pellinghelli, M. A.; Tiripicchio, A. *Organometallics* **2000**, *19*, 3161.
(13) Royo, P.; Sánchez-Nieves, J. *J. Organomet. Chem.* **2000**, *597*, 61.
(14) Royo, P.; Sánchez-Nieves, J.; Pellinghelli, M. A.; Tiripicchio, A. *J. Organomet. Chem.* **1998**, *563*, 15.
(15) Gavenonis, J.; Tilley, T. D. *Organometallics* **2004**, *23*, 31.
(16) Antinolo, A.; Fajardo, M.; Otero, A.; Prashar, S. *Eur. J. Inorg. Chem.* **2003**, 17.
(17) Feng, S. G.; Roof, G. R.; Chen, E. Y. X. *Organometallics* **2002**, *21*, 832.
(18) Coles, M. P.; Dalby, C. I.; Gibson, V. C.; Little, I. R.; Marshall, E. L.; da Costa, M. H. R.; Mastroianni, S. *J. Organomet. Chem.* **1999**, *591*, 78.
(19) Antonelli, D. M.; Leins, A.; Stryker, J. M. *Organometallics* **1997**, *16*, 2500.

10.1021/om701068h CCC: $40.75
Publication on Web 03/04/2008

copolymers[24–30] are essential features of the polymerization of methacrylates by transition-metal complexes. Group 3 and 4 metallocene complexes have been widely explored over the past few years and, more recently,[24–36] tantalum cyclopentadienyl based complexes have also emerged as active catalysts for MMA polymerization.[17,37,38] Different mechanisms based on group transfer polymerization have been proposed, involving mononuclear or dinuclear alkyl or enolate active species and depending on the cocatalyst employed, mainly $E(C_6F_5)_3$ (E = B, Al). However, MMA polymerization has also been described for group 4 imido metallocene complexes in the presence of $Al(C_6F_5)_3$, involving the formation of an oxametallacycle by addition of MMA to the metal−nitrogen multiple bond and further generation of a zwitterionic dinuclear enol aluminate intermediate by rupture of the metal–oxygen bond produced by $Al(C_6F_5)_3$.[39]

In this work, we have extended our initial interest in half-sandwich imido neutral $[MCp(NR)X_2]$ (M = group 5 metal)[9–14,40–44] and cationic monocyclopentadienyl group 5 metal complexes[45,46] to noncyclopentadienyl imido complexes of the type $[MBz_2(NR)X]$ (M = Nb, Ta; X = Bz, OAr), with the aim of synthesizing cationic derivatives by reaction with the Lewis acids $E(C_6F_5)_3$ (E = B, Al) and exploring their activity as MMA polymerization catalysts. Initial studies related to the tribenzyl compounds (X = Bz) have also been extended to the aryloxo derivatives (X = OAr) in order to modify their reactivity and to stabilize these types of high-valent cationic compounds.

Scheme 1[a]

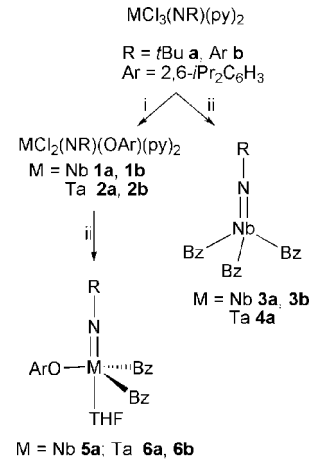

[a] Legend: (i) LiOAr; (ii) BzMgCl.

Recently, Bergman et al. have reported the synthesis of the tantalum tribenzyl derivative $[Ta(NtBu)Bz_3]$,[47] which in the presence of the Lewis acids $B(C_6F_5)_3$ and $[Ph_3C][B(C_6F_5)_4]$ generates the corresponding zwitterionic and ion-unpaired derivatives that were applied as catalysts for the hydroamination of acetylenes.

Furthermore, considering the isolobal relationship between the imido and cyclopentadienyl ligands,[1] a similar relation could be established between the non-cyclopentadienyl imido complexes $[MX_3(NR)]$ (M = group 5 metal) and monocyclopentadienyl complexes $[MCpX_3]$ (M = group 4 metal). This last type of complex has found widespread application as an olefin polymerization catalyst, including MMA,[25,48] and thus comparative chemical and DFT studies have also been carried out in this work.

Results and Discussion

Synthesis of Neutral Compounds. Following the procedure previously reported by Wigley et al. for the synthesis of $[TaCl_2(NAr)(OAr)(py)_2]$ (Ar = 2,6-*i*Pr$_2$C$_6$H$_3$)[49] by reaction of the trichloro complexes with LiOAr, we have isolated the new imido aryloxo compounds $[MCl_2(NR)(OAr)(py)_2]$ (M = Nb, R = *t*Bu (**1a**), Ar (**1b**); M = Ta, R = *t*Bu (**2a**)) in good yields, using the respective trichloro imido derivatives $[MCl_3(NR)(py)_2]$ (M = Nb, R = *t*Bu, Ar; M = Ta, R = *t*Bu)[49,50] as source materials (Scheme 1). All of these new complexes retained the original two molecules of pyridine coordinated to the metal center, whichever imido substituent was used.

The trichloro imido compounds $[NbCl_3(NR)(py)_2]$ (R = *t*Bu, Ar) and the aryloxo imido compounds **1** and **2a** were transformed into the benzyl derivatives $[NbBz_3(NR)]$ (R = *t*Bu (**3a**), Ar (**3b**)) and $[MBz_2(NR)(OAr)(THF)]$ (M = Nb, R = *t*Bu (**5a**); M = Ta, R = *t*Bu (**6a**), Ar (**6b**)), respectively, after addition of the corresponding molar amounts of [BzMgCl] (Scheme 1). The synthesis of the aryloxo complexes **5a** and **6a** required addition of stoichiometric amounts of [BzMgCl] to prevent formation of the corresponding tribenzyl derivatives $[MBz_3(NR)]$, which

(20) Anderson, L. L.; Arnold, J.; Bergman, R. G. *Org. Lett.* **2004**, *6*, 2519.
(21) Ong, T. G.; Yap, G. P. A.; Richeson, D. S. *Chem. Commun.* **2003**, 2612.
(22) Burland, M. C.; Pontz, T. W.; Meyer, T. Y. *Organometallics* **2002**, *21*, 1933.
(23) Blake, R. E.; Antonelli, D. M.; Henling, L. M.; Schaefer, W. P.; Hardcastle, K. I.; Bercaw, J. E. *Organometallics* **1998**, *17*, 718.
(24) Strauch, J. W.; Faure, J. L.; Bredeau, S.; Wang, C.; Kehr, G.; Frohlich, R.; Luftmann, H.; Erker, G. *J. Am. Chem. Soc.* **2004**, *126*, 2089.
(25) Chen, E. Y. X. *J. Polym. Sci., Part A: Polym. Chem.* **2004**, *42*, 3395.
(26) Batis, C.; Karanikolopoulos, G.; Pitsikalis, M.; Hadjichristidis, N. *Macromolecules* **2003**, *36*, 9763.
(27) Chen, E. Y. X.; Cooney, M. J. *J. Am. Chem. Soc.* **2003**, *125*, 7150.
(28) Bolig, A. D.; Chen, E. Y. X. *J. Am. Chem. Soc.* **2002**, *124*, 5612.
(29) Boffa, L. S.; Novak, B. M. *Chem. Rev.* **2000**, *100*, 1479.
(30) Yasuda, H.; Yamamoto, H.; Yamashita, M.; Yokota, K.; Nakamura, A.; Miyake, S.; Kai, Y.; Kanehisa, N. *Macromolecules* **1993**, *26*, 7134.
(31) Lian, B.; Lehmann, C. W.; Navarro, C.; Carpentier, J. F. *Organometallics* **2005**, *24*, 2466.
(32) Stojcevic, G.; Kim, H.; Taylor, N. J.; Marder, T. B.; Collins, S. *Angew. Chem., Int. Ed.* **2004**, *43*, 5523.
(33) Frauenrath, H.; Keul, H.; Hocker, H. *Macromolecules* **2001**, *34*, 14.
(34) Cameron, P. A.; Gibson, V. C.; Graham, A. J. *Macromolecules* **2000**, *33*, 4329.
(35) Yasuda, H. *J. Organomet. Chem.* **2002**, *647*, 128.
(36) Yasuda, H. *J. Polym. Sci., Part A: Polym. Chem.* **2001**, *39*, 1955.
(37) Mariott, W. R.; Gustafson, L. O.; Chen, E. Y. X. *Organometallics* **2006**, *25*, 3721.
(38) Matsuo, Y.; Mashima, K.; Tani, K. *Angew. Chem., Int. Ed.* **2001**, *40*, 960.
(39) Jin, J. Z.; Mariott, W. R.; Chen, E. Y. X. *J. Polym. Sci., Part A: Polym. Chem.* **2003**, *41*, 3132.
(40) Nicolás, P.; Royo, P. *Inorg. Chim. Acta* **2005**, *358*, 1494.
(41) Alcalde, M. I.; Gómez-Sal, M. P.; Royo, P. *Organometallics* **2001**, *20*, 4623.
(42) Alcalde, M. I.; Gómez-Sal, M. P.; Royo, P. *Organometallics* **1999**, *18*, 546.
(43) Alcalde, M. I.; Gómez-Sal, P.; Martín, A.; Royo, P. *Organometallics* **1998**, *17*, 1144.
(44) Gómez, M.; Gómez-Sal, P.; Jiménez, G.; Martín, A.; Royo, P.; Sánchez-Nieves, J. *Organometallics* **1996**, *15*, 3579.
(45) Sánchez-Nieves, J.; Royo, P. *Organometallics* **2007**, 2880.
(46) Sánchez-Nieves, J.; Royo, P.; Mosquera, M. E. G. *Organometallics* **2006**, *25*, 2331.
(47) Anderson, L. L.; Schmidt, J. A. R.; Arnold, J.; Bergman, R. G. *Organometallics* **2006**, *25*, 3394.
(48) Jensen, T. R.; Yoon, S. C.; Dash, A. K.; Luo, L. B.; Marks, T. J. *J. Am. Chem. Soc.* **2003**, *125*, 14482.
(49) Chao, Y. W.; Wexler, P. A.; Wigley, D. E. *Inorg. Chem.* **1989**, *28*, 3860.
(50) Korolev, A. V.; Rheingold, A. L.; Williams, D. S. *Inorg. Chem.* **1997**, *36*, 2647.

were observed when working with an excess resulting from the simultaneous substitution of the aryloxo group. This side reaction could be responsible for the lower yields obtained in the synthesis of complexes **5a** and **6** with respect to those observed for complexes **3** and $[TaBz_3(NtBu)]$[47] (**4a**). The yields of these reactions also reflected the different electronic stabilizations provided by the two different types of imido groups. When R was *t*Bu, the yields were moderate to good, whereas rather poor yields were obtained when R was Ar and in the particular case of the complexes $[TaCl_3(NAr)(py)_2]$ and $[NbCl_2(NAr)(OAr)(THF)]$ (**1b**) none of the benzyl derivatives could be observed.

The ^1H and ^{13}C NMR spectra of the tribenzyl imido compounds **3a**,**b** showed only one resonance for the three equivalent benzyl ligands. The $^1J_{C-H}$ value of the methylene group (ca. 133 Hz) and the chemical shift of the ipso carbon of the phenyl ring ($\delta \sim 138$) suggested η^2 coordination of the benzyl ligand,[47,51,52] which was confirmed by X-ray diffraction studies (vide infra). The same spectroscopic parameters were observed for the tantalum complex $[TaBz_3(NtBu)]$ (**4a**).[47]

The elemental analysis of **5a** and **6a**,**b** were consistent with the proposed chemical formulas, and their ^1H and ^{13}C NMR spectra demonstrated coordination of THF to a metal center bound to two equivalent benzyl ligands, with the diastereotopic methylene protons observed as a pair of doublets in the ^1H NMR spectrum. The $^1J_{C-H}$ value of the methylene group (ca. 120 Hz) and the chemical shift of the ipso carbon ($\delta \sim 145$) of the benzyl ligands were consistent with their η^1 coordination. These structural features are consistent with a trigonal-bipyramidal geometry in which the strong donor imido and THF ligands occupy the axial positions, whereas the aryloxo and two benzyl ligands are located in the equatorial positions. This structure was supported by the results of NOE experiments.

The metal centers of these imido complexes show different coordination numbers. The trichloro and dichloroaryloxo derivatives **1** and **2a** are 18-electron pseudooctahedral compounds with two additional pyridine ligands, considering the aryloxo and imido ligands as 3- and 4-electron donors, respectively. However, considering the benzyl ligand as a 1-electron donor, the dibenzylaryloxo derivatives **5a** and **6** with one additional THF molecule are 16-electron trigonal bipyramidal species and the ligand-free neutral tribenzyl **3** and **4a** are 12-electron compounds with a pseudotetrahedral geometry.

Surprisingly, neither the steric hindrance nor the strong σ and π donor character of the aryloxo ligand in the imido complexes **5** and **6a** prevented the coordination of one additional neutral THF ligand, whereas the tribenzyl imido complexes **3** and **4a** did not coordinate additional ligands. Furthermore, the cis coordination of the imido and aryloxo ligands was expected to maximize the overlapping of the π orbitals of these ligands with the metal center.[49] Apparently, the σ donating ability and the η^2 coordination of the three benzyl groups weaken the interaction of the metal center with the neutral donor ligand in compounds **3** and **4a**, facilitating the dissociation of this ligand, which is removed after washing with hexane and drying under vacuum for a few hours.

X-ray Structure of 3a. Crystals suitable for X-ray diffraction studies were obtained for the tribenzyl imido compound $[NbBz_3(NtBu)]$ (**3a**). The molecular structure of **3a** is shown in Figure 1, and a selection of bond distances and angles is

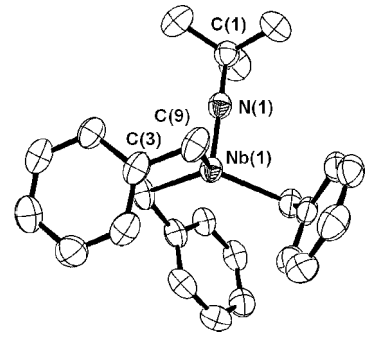

Figure 1. ORTEP diagram of $[NbBz_3(NtBu)]$ (**3a**). Hydrogen atoms have been omitted, and thermal ellipsoids are shown at the 50% level.

Table 1. Selected Bond Lengths (Å) and Angles (deg) for the Compounds $[MBz_3(NtBu)]$ (M = Nb (3a), Ta[47])

	M = Nb	M = Ta
M−N	1.747(4)	1.737(6)
M−C(9)	2.245(3)	2.216(4)
M−C(3)	2.679(3)	2.678
M−N−C(1)	180.00(1)	180.00
M−C(3)−C(9)	89.62(17)	90.80(3)
N−M−C(9)	98.26(9)	100.0(1)
C(9)−M−C(9)	117.97(4)	117.06(7)

presented in Table 1. Complex **3a** exhibits a C_{3v} pseudotetrahedral structure, which resembles that found in typical monocyclopentadienyl three-legged piano-stool derivatives, with three narrower N−Nb−C and three more open C−Nb−C angles. The bond length and bond angle values were very close to those found in the analogous tantalum derivative $[TaBz_3(NtBu)]$ (Table 1). The three $Nb-C_{ipso}$ distances (2.679(3) Å) and the three $Nb-C-C_{ipso}$ angles (89.62(2)°) are clearly indicative of η^2-benzyl coordination. Although this η^2 interaction is well represented for electron-deficient metal−benzyl compounds,[53–59] the presence of three equivalent η^2-benzyl ligands is unusual, probably as a consequence of the coordinative requirements of the metal atom, in comparison with those of the related zirconium cyclopentadienyl derivative $[ZrCpBz_3]$.[60] Finally, the Nb−N bond distance (1.747(4) Å) is in the range expected for a Nb−N triple bond, in accordance with the linearity observed for the Nb−N−C bond angle (180.00(1)°).[1]

Synthesis of Zwitterionic Compounds. The reactions of the tribenzyl derivatives $[MBz_3(NtBu)]$ (M = Nb (**3a**), Ta (**4a**)) with the Lewis acids $E(C_6F_5)_3$ (E = B, Al) afforded the zwitterionic compounds $[MBz_2(NtBu)\{\eta^6\text{-}C_6H_5CH_2E(C_6F_5)_3\}]$ (M = Nb, E = B (**7a-B**), Al (**7a-Al**); M = Ta, E = Al (**8a-Al**)) (Scheme 2). All of these new complexes were soluble in C_6D_6. Formation of the hypothetical niobium compounds $[NbBz_2(NAr)\{\eta^6\text{-}C_6H_5CH_2E(C_6F_5)_3\}]$ in similar reactions with the arylimido

(51) Gauvin, R. M.; Osborn, J. A.; Kress, J. *Organometallics* **2000**, *19*, 2944.
(52) Latesky, S. L.; McMullen, A. K.; Niccolai, G. P.; Rothwell, I. P.; Huffman, J. C. *Organometallics* **1985**, *4*, 902.
(53) Prashar, S.; Fajardo, M.; Garcés, A.; Dorado, I.; Antiñolo, A.; Otero, A.; López-Solera, I.; López-Mardomingo, C. *J. Organomet. Chem.* **2004**, *689*, 1304.
(54) Groysman, S.; Goldberg, I.; Kol, M.; Goldschmidt, Z. *Organometallics* **2003**, *22*, 3793.
(55) Thorn, M. G.; Lee, J.; Fanwick, P. E.; Rothwell, I. P. *Dalton Trans.* **2002**, 3398.
(56) Schweiger, S. W.; Salberg, M. M.; Pulvirenti, A. L.; Freeman, E. E.; Fanwick, P. E.; Rothwell, I. P. *Dalton Trans.* **2001**, 2020.
(57) Murphy, V. J.; Turner, H. *Organometallics* **1997**, *16*, 2495.
(58) Ciruelo, G.; Cuenca, T.; Gómez, R.; Gómez-Sal, P.; Martín, A.; Rodríguez, G.; Royo, P. *J. Organomet. Chem.* **1997**, *547*, 287.
(59) Álvaro, L. M.; Cuenca, T.; Flores, J. C.; Royo, P.; Pellinghelli, M. A.; Tiripicchio, A. *Organometallics* **1992**, *11*, 3301.
(60) Scholz, J.; Rehbaum, F.; Thiele, K. H.; Goddard, R.; Betz, P.; Kruger, C. *J. Organomet. Chem.* **1993**, *443*, 93.

Scheme 2. Reaction of Tribenzyl Imido Complexes with the Lewis Acids $E(C_6F_5)_3$ (E = B, Al)

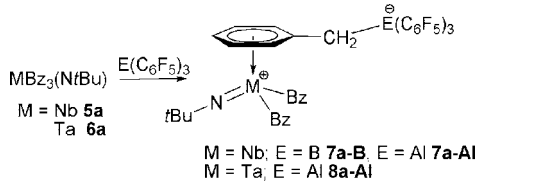

derivative **3b** were unsuccessful, in accordance with the σ-donor capacity of the arylimido ligand being lesser than that of the related *tert*-butylimido ligand.

The ^{1}H and ^{13}C NMR spectra of complexes **7** and **8** showed similar patterns which were also analogous to that reported for $[TaBz_2(NtBu)\{\eta^6\text{-}C_6H_5CH_2B(C_6F_5)_3\}]$ (**8a-B**).[47] The C_s symmetry of complexes **7** and **8** gave rise to the three resonances observed in the ^{1}H NMR spectra for the AA′BB′C spin system of the η^6-C_6H_5 ring and the two doublets for the diastereotopic M−CH_2 protons of the two equivalent benzyl ligands. The values found for $^1J_{C-H}$ of the benzyl methylene group and for the chemical shift of the ipso carbon atom of the phenyl ring were very close to those found for the starting $[MBz_3(NtBu)]$ complexes, indicating a similar η^2 coordination. Formation of the $[C_6H_5CH_2E(C_6F_5)_3]^-$ anion moiety was indicated by a broad signal observed at about 3 ppm for the Bz−E groups. Coordination of the anionic benzylborate phenyl ring to the metal center was in agreement with the upfield shift of three resonances with respect to those expected for a normal phenyl ring, although such displacement was not observed for the related zirconium complexes $[ZrCpBz_2\{\eta^6\text{-}C_6H_5CH_2E(C_6F_5)_3\}]$ (E = B,[61] Al (vide infra)). We believe that this different behavior could be attributed to slippage of the phenyl ring in complexes **7** and **8**, as has been confirmed by the DFT calculations discussed below. Finally, the presence of the ion-pair interaction for the benzylborate complex **7a-B** was confirmed by means of the $\delta_{meta}-\delta_{para}$ difference of about 4 ppm observed in its ^{19}F NMR spectrum.

In addition, the reactivity toward Lewis acids was studied for the aryloxo imido compounds $[MBz_2(NR)(OAr)(THF)]$ (M = Nb, R = *t*Bu (**5a**); M = Ta, R = *t*Bu (**6a**), Ar (**6b**)). However, only the tantalum derivative **6a** reacted successfully with the Lewis acids $E(C_6F_5)_3$ (E = B, Al) (Scheme 3). Addition of 1 equiv of $B(C_6F_5)_3$ to a C_6D_6 solution of **6a** gave an insoluble reddish oil, which after being redissolved in BrC_6D_5 was characterized by NMR spectroscopy as the ionic compound $[TaBz(NtBu)(OAr)(THF)][BzB(C_6F_5)_3]$ (**9a**). The ^{1}H NMR of **9a** showed one broad resonance for the methylene protons of the benzyl−B group at about δ 3.20, two multiplets due to the coordinated THF, and two doublets corresponding to the methylene protons CH_2−Nb of the niobium-bonded benzyl group. In addition, three resonances due to the $[BzB(C_6F_5)_3]^-$ anion were observed in the ^{19}F NMR spectrum with a value of 2.8 ppm for the $\delta_{meta}-\delta_{para}$ difference, indicating that the ion-pair interaction[62] does not exist. Addition of another 1 equiv of $B(C_6F_5)_3$ to **9a** produced the abstraction of THF, leading to formation of the zwitterionic complex $[TaBz(NtBu)(OAr)\{\eta^6\text{-}C_6H_5CH_2B(C_6F_5)_3\}]$ (**11a-B**), with elimination of the $(THF)\cdot B(C_6F_5)_3$ adduct and concomitant η^6 coordination of the C_6H_5 ring of the $[BzB(C_6F_5)_3]^-$ anion. The same transformation

Scheme 3. Reaction of Dibenzyl Aryloxo Imido Complexes with the Lewis Acids $E(C_6F_5)_3$ (E = B, Al)[a]

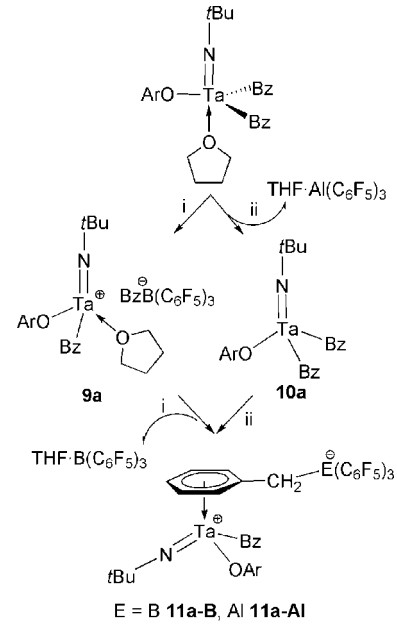

[a] Legend: (i) $B(C_6F_5)_3$; (ii) $Al(C_6F_5)_3$.

directly into **11a-B** can be obtained by addition of 2 equiv of $B(C_6F_5)_3$ to the starting compound **6a**.

The first step of the similar reaction of **6a** with $Al(C_6F_5)_3$ was the elimination of the neutral $(THF)\cdot Al(C_6F_5)_3$ adduct with formation of the neutral THF-free tantalum complex $[TaBz_2(NR)(OAr)]$ (**10a**), which was also characterized by NMR spectroscopy. Clearly, the higher oxophilicity of Al vs B was responsible for this different reaction pathway. Furthermore, the formation of the THF-free compound **10a** from **6a** demonstrated that coordination of the THF ligand stabilizes the aryloxo compounds **5** and **6** with respect to the less electron-deficient tribenzyl derivatives **3** and **4**, although it is not an essential requirement for their isolation. This fact could suggest that the benzyl ligand is a better σ donor ligand than the aryloxo ligand. The ^{1}H and ^{13}C NMR spectroscopic data of **10a** were very close to those observed for **6a**, with slight shifts of the whole set of resonances. Addition of another 1 equiv of $Al(C_6F_5)_3$ produced the abstraction of one of the benzyl ligands to give the corresponding zwitterionic compound $[TaBz(NtBu)(OAr)\{\eta^6\text{-}C_6H_5CH_2Al(C_6F_5)_3\}]$ (**11a-Al**), which showed a ^{1}H and ^{13}C NMR pattern similar to that observed for **11a-B**. Furthermore, the three resonances corresponding to the $[\eta^6\text{-}C_6H_5CH_2Al(C_6F_5)_3]^-$anion at δ −121.6 (F_{ortho}), −149.9 (F_{para}), and −159.4 (F_{meta}) were observed in the ^{19}F NMR spectrum.

In contrast to the ionic compound **9a** containing the free borate anion, the new zwitterionic compounds **11a-B** and **11a-Al** were soluble in C_6D_6. The interaction proposed for the $[\eta^6\text{-}C_6H_5CH_2E(C_6F_5)_3]^-$ anions (E = B, Al) in both complexes was confirmed by the upfield shifted C_6H_5 resonances observed in their ^{1}H NMR spectra. Furthermore, the ^{19}F NMR spectrum of **11a-B** showed a higher value of ca. 4.0 ppm for the $\delta_{meta}-\delta_{para}$ difference, in accordance with the presence of a strong ion-pairing interaction,[62] whereas three resonances corresponding to the $[\eta^6\text{-}C_6H_5CH_2Al(C_6F_5)_3]^-$ anion at δ −121.6 (F_{ortho}), −149.9 (F_{para}), and −159.4 (F_{meta}) were observed in the ^{19}F NMR spectrum of **11a-Al**.

The reactivity described here for these group 5 metal imido complexes resembles that reported for the zirconium derivative

(61) Pellecchia, C.; Immirzi, A.; Grassi, A.; Zambelli, A. *Organometallics* **1993**, *12*, 4473.

(62) Horton, A. D.; de With, J.; van der Linden, A. J.; van der Weg, H. *Organometallics* **1996**, *15*, 2672.

Scheme 4. Reaction of the Zirconium Tribenzyl Monocyclopentadienyl Complex with Lewis Acids $E(C_6F_5)_3$ (E = B, Al)

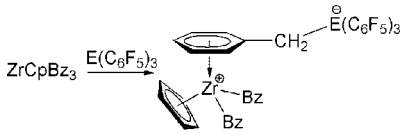

E = B **12-B**, Al **12-Al**

[$ZrCpBz_3$], which also yielded the analogous zwitterionic η^6-arene compound [$ZrCpBz_2\{\eta^6$-$C_6H_5CH_2B(C_6F_5)_3\}$] (**12-B**), when reacting with $B(C_6F_5)_3$.[61] In view of these results, we decided to complete our previous studies investigating the related reaction of [$ZrCpBz_3$] with $Al(C_6F_5)_3$ (Scheme 4). The reaction was carried out in C_6D_6 and monitored by NMR spectroscopy at ambient temperature to give the expected zwitterionic complex [$ZrCpBz_2\{\eta^6$-$C_6H_5CH_2Al(C_6F_5)_3\}$] (**12-Al**), which was characterized by NMR spectroscopy. The ^{1}H spectrum showed broad signals resulting from the formation of **12-Al**, and the ^{19}F NMR spectrum presented three resonances corresponding to the [η^6-$C_6H_5CH_2Al(C_6F_5)_3]^-$ anion. However, the ^{1}H NMR spectrum obtained from a similar experiment in CD_2Cl_2 at −70 °C clearly showed three multiplets corresponding to the η^6-coordinated phenyl ring of the benzylborate anion and two doublets for the diastereotopic methylene protons of the metal-bound benzyl ligands. The most remarkable difference from the related group 5 metal compounds is that the $^1J_{C-H}$ value of the Zr−CH_2 group (122 Hz) and the chemical shift of the phenyl ipso carbon of this benzyl ligand (δ 148.5) show the typical values expected for η^1-coordinated benzyl ligands in contrast to the η^2 interaction found for the group 5 metal imido derivatives **7** and **8**, probably due to the bulkiness of the cyclopentadienyl ligand.

Theoretical Calculations. Optimized geometries of the most stable conformers for the complexes [$NbMe_2(NtBu)\{\eta^6$-$C_6H_5CH_2B(C_6F_5)_3\}$] (**I**) and [$ZrMe_2Cp\{\eta^6$-$C_6H_5CH_2B(C_6F_5)_3\}$] (**II**) are shown in Figure 2, and calculated values of bond distances and angles are collected in Table 2. These complexes are models for the zwitterionic compounds [$NbBz_2(NtBu)\{\eta^6$-$C_6H_5CH_2B(C_6F_5)_3\}$] (**7a-B**) and [$ZrCpBz_2\{\eta^6$-$C_6H_5CH_2B(C_6F_5)_3\}$] (**12-B**), respectively, where the benzyl groups were replaced by methyl ligands. The complexes show a pseudotetrahedral arrangement of ligands around the metal center. The calculated Nb−N distance (1.743 Å) and Nb−N−C angle (180.0°) are consistent with a Nb≡N triple bond, and they are essentially the same as those experimentally found for the similar complex **3a** (1.748 Å and 180.0° in Figure 1, respectively). The spatial orientation of the arene ligand with respect to the metal fragment in both complexes can be defined using the N−Nb−X−C1 and X2−Zr−X1−C1 dihedral angles (where X stands for the centroid of the different rings). As can be seen in Figure 2, the spatial positions of the arene ligand are roughly the same for both complexes (64.8 and 64.1° for complexes **I** and **II**, respectively). The distance between the metal atom and the arene centroid is slightly longer for complex **II** (2.302 versus 2.269 Å). The Nb−C_{arene} distances can be grouped in two sets, one with short distances Nb−C1, Nb−C2, and Nb−C3 (2.646, 2.521, and 2.567 Å, respectively) and other set of long distances Nb−C4, Nb−C5, and Nb−C6 (2.721, 2.814, and 2.742 Å, respectively). However, the Zr−C_{arene} distances are closer to each other. Furthermore, the standard deviation of the distances between the metal center and the carbon atoms belonging to the arene ligand (0.111 and 0.026 Å for complexes **I** and **II**, respectively) indicate a less symmetric coordination of the arene ligand to the metal fragment for complex **I** with respect to complex **II**. In Table 2, a comparison of the geometry of

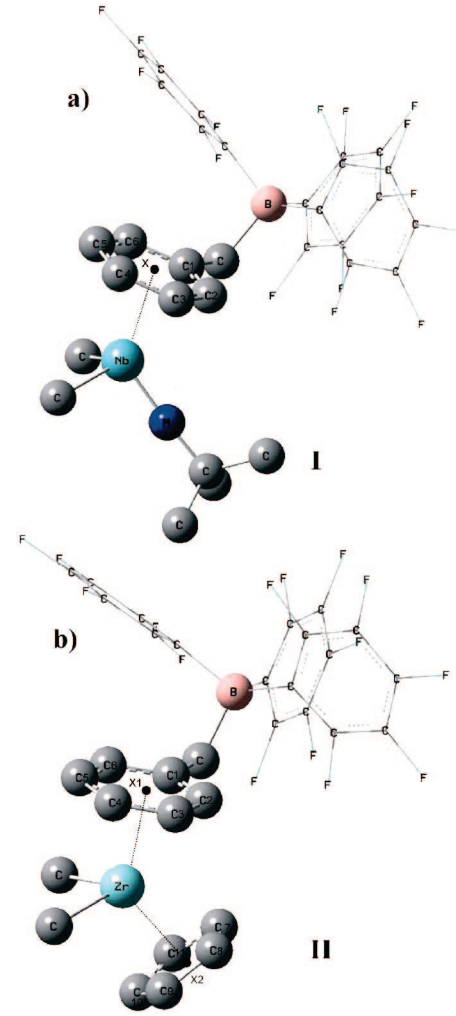

Figure 2. DFT-optimized geometries of the complexes (a) [$NbMe_2(NtBu)\{\eta^6$-$C_6H_5CH_2B(C_6F_5)_3\}$] (**I**) and (b) [$ZrMe_2Cp\{\eta^6$-$C_6H_5CH_2B(C_6F_5)_3\}$] (**II**).

Table 2. Calculated Values of Bond Distances (Å) and Angles (deg) of the Complexes [$NbMe_2(NtBu)\{\eta^6$-$C_6H_5CH_2B(C_6F_5)_3\}$] (I) and [$ZrMe_2Cp\{\eta^6$-$C_6H_5CH_2B(C_6F_5)_3\}$] (II)[a]

	M = Nb	M = Zr	M = Zr[b]
Nb−N	1.742		
Zr−X2		2.200	2.180
M−Me	2.166	2.258	
	2.170	2.260	
M−X1	2.269	2.302	2.300
M−C1	2.646	2.719	2.860
M−C2	2.521	2.668	2.730
M−C3	2.567	2.663	2.610
M−C4	2.721	2.702	2.663
M−C5	2.814	2.726	2.680
M−C6	2.742	2.707	2.740
C−B	1.690	1.687	1.690
C1−B	1.470	1.472	1.490
C1−C−B	113.8	114.2	112.0
X1−Zr−X2		133.1	126.0
N−Nb−X	126.5		
X2−Zr−X1−C1		64.1	
N−Nb−X−C1	64.8		

[a] X stands for the position of the centroid in the corresponding ring, X1 for η^6-$C_6H_5CH_2B$, and X2 for η^5-C_5H_5. [b] Experimental values for [$ZrBz_2Cp\{\eta^6$-$C_6H_5CH_2B(C_6F_5)_3\}$].[61]

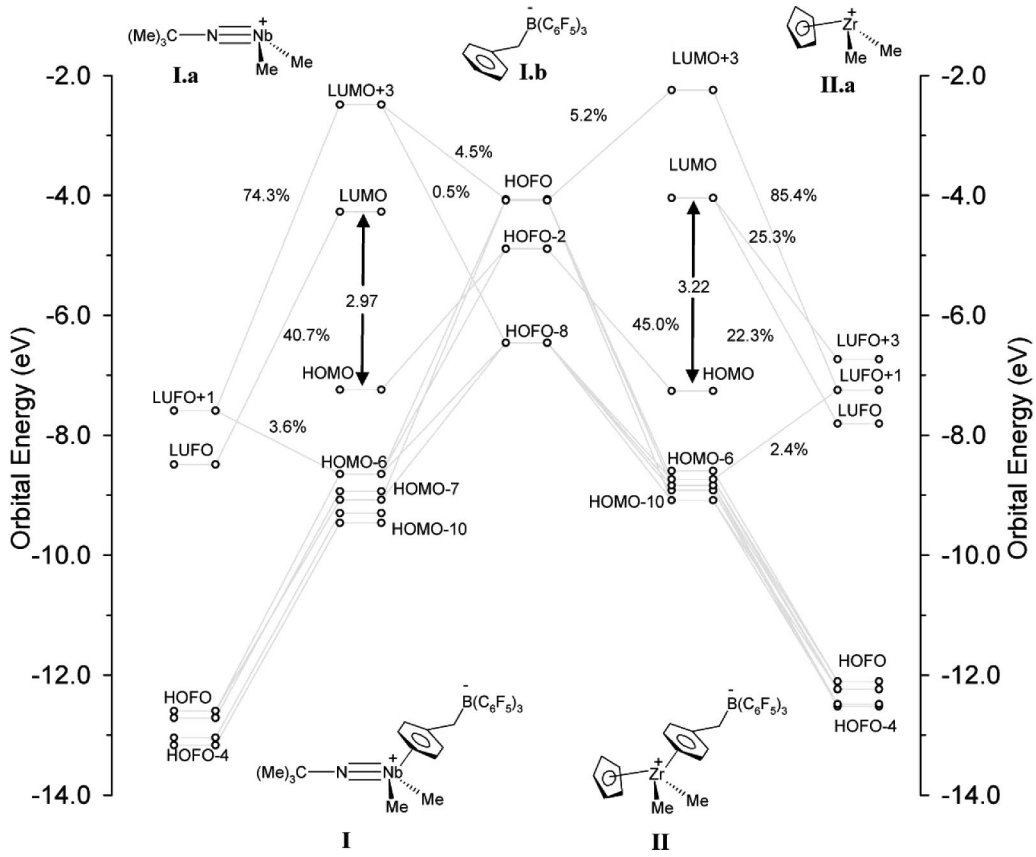

Figure 3. Molecular orbital diagram for the formation of complexes **I** and **II** from the corresponding fragments.

complex **II** and the structure obtained by Pellecchia et al. for the zwitterionic complex [ZrBz$_2$Cp{η^6-C$_6$H$_5$CH$_2$B(C$_5$F$_5$)$_3$}] is given.[61] In general, the experimental and calculated structures are quite similar; only differences of around 0.1 Å and 5° in distances and angles, respectively, are observed.

Frontier Orbitals of Complexes I and II. In order to gain further insight into the metal–ligand bonding, a fragment molecular orbital approach is applied to establish the frontier orbitals of complexes **I** and **II**. Thus, the [NbMe$_2$(N*t*Bu){η^6-C$_6$H$_5$CH$_2$B(C$_6$F$_5$)$_3$}] complex (**I**) can be seen as being formed by two different fragments, the cationic fragment [NbMe$_2$(N*t*Bu)]$^+$ (**I.a**) and the anionic fragment [C$_6$H$_5$CH$_2$B(C$_6$F$_5$)$_3$]$^-$ (**I.b**), respectively. Similarly, [ZrMe$_2$Cp{η^6-C$_6$H$_5$CH$_2$B(C$_6$F$_5$)$_3$}] complex (**II**) is made from the component fragments [ZrCpMe$_2$]$^+$ (**II.a**) and [C$_6$H$_5$CH$_2$B(C$_6$F$_5$)$_3$]$^-$ (**I.b**), respectively.

The LUFO (lowest unoccupied fragment orbital) and LUFO+1 from fragment **I.a** are essentially pure d_{z^2} and $d_{x^2-y^2}$ orbitals from the metal, respectively. Other unoccupied LUFOs for **I.a** are antibonding π^* orbitals arising from the interaction between d_{xz}, d_{yz}, and d_{xy} metal orbitals and occupied π orbitals of the imido group, fundamentally p_x, p_y, and p_z orbitals from the nitrogen atom. The corresponding occupied π orbitals for the metal−imido bond, HOFO, HOFO+1, and HOFO+3 (highest occupied fragment orbital), show a clear bonding character arising from the interaction between Nb d and N p atomic orbitals. Frontier molecular orbitals for the **II.a** fragment are quite similar to those in fragment **I.a**. The HOFO and HOFO+1 orbitals for the **I.b** fragment have π^* character on the benzyl ring.

A simplified molecular orbital correlation diagram is depicted in Figure 3. The isolobal and isoelectronic character of both complexes is clear, although some differences are observed. The LUMO orbital for complex **I** arises mainly from the interaction between the empty LUFO **I.a** (40.7%), which is mainly a d_{z^2} orbital, and LUFO+3 **I.b** (11.9%) with a small contribution of the HOFO **I.b** (2.0%). The total Mülliken overlap population for this orbital is −0.008e which indicates a slightly antibonding character for this MO. For complex **II**, the corresponding LUMO orbital rises from mixing LUFO+3 **II.a** ($d_{x^2-y^2}$, 22.3%) and LUFO **II.a** (d_{z^2}, 25.3%) with the LUFO+3 **I.b** (17.3%) orbital but without the participation of the HOFO **I.b**. The Mülliken overlap population for the LUMO of complex **II** has a value of 0.055e. In contrast, LUMO orbital energies in both complexes are rather similar (−4.27 and −4.04 eV for complexes **I** and **II**, respectively). Hence, a donor molecule might yield a more stable donor–acceptor bond in complex **II** due to the bonding character of the LUMO orbital.

Another important ligand-to-metal interaction between the fragments defined above in both complexes arises from the interaction between HOFO **I.a** (HOFO **I.b**), LUFO+1 **I.a** (LUFO **I.b**), and HOFO **I.b** orbitals giving predominantly the LUMO+3 and HOMO-6 molecular orbitals in complexes **I** (**II**). The character of LUMO+3 is strongly antibonding for both complexes (−0.220e and −0.516e for complexes **I** and **II**, respectively), while for HOMO-6 a slightly antibonding character is observed (−0.016e and −0.005 e for complexes **I** and **II**, respectively), probably due to the repulsive interaction between HOMO orbitals of the two fragments. The interaction between the HOFO and HOFO-8 of fragment **I.b** with HOFO-0−HOFO-4 for both metal fragments gives an increase in energy (destabilization) of the molecular orbital responsible of Nb-imido and Zr-Cp bonds (HOMO-7–HOMO-10 set in Figure 3).

Finally, the total Mülliken overlaps for complexes **I** and **II** are positive (0.240e and 0.208 e, respectively,) pointing to a stable interaction between fragments.

Table 3. Polymerization of MMA with Imido Complexes using $E(C_6F_5)_3$ (E = B, Al) as Cocatalyst[a]

run	[M]	E	T (°C)	t (h)	yield (%)	M_w/M_n[b]	$10^4 M_n$	10^4 M_n(calcd)[c]	rr (%)[d]	mr (%)[d]	mm (%)[d]
1	**3a**	Al	−40	5	37	1.25	2.03	0.76	60	34	6
2[e]	**3a**	Al	0	5	30	2.08	2.93	0.76	72	27	2
3	**3a**	Al	0	5	40	1.28	2.01	0.76	62	33	7
4	**3a**	Al	25	16	50	1.35	2.01	1.04	70	23	7
5	**6a**	B	25	16	14	1.47	5.21	0.29	61	32	7
6	**6a**	Al	40	5	10	1.47	3.84	0.21	58	33	9

[a] Polymerization conditions: Complex [M] (4.8×10^{-5} mol) and $E(C_6F_5)_3$ (9.6×10^{-5} mol) premixed in toluene (3 mL), then MMA (1 g; [MMA]:[M] = 206:1). [b] Determined by GPC in THF vs polystyrene standards. [c] M_n(calcd) values = conv × [MMA]/[M] × 100.81 (100.81 is the formula weight of MMA); [d] Determined by ^{1}H NMR in $CDCl_3$. [e] CH_2Cl_2.

Formation Energies for Complexes I and II. Electronic formation energies of the complexes **I** and **II**, with respect to the isolated fragments, are −117.0 and −113.8 kcal/mol, reflecting the exergonic nature of the bond between them. The stabilization energy for complex **I** is 3.2 kcal/mol higher than that corresponding to complex **II**, indicating a more difficult separation of the ionic pair for complex **I** with respect to complex **II**.

MMA Polymerization. The niobium tribenzyl imido complex [$NbBz_3$(N*t*Bu)] (**3a**) activated by addition of 2.0 equiv of $Al(C_6F_5)_3$ showed rather low catalytic activity for MMA polymerization, whereas only traces of PMMA were observed when the isolobal zirconium derivative [$ZrCpBz_3$] was used for comparison and when the related niobium imido (**3b**) and tantalum imido (**4**) complexes were studied under similar conditions. In contrast, no activation was observed for any of these compounds when $B(C_6F_5)_3$ was used as the Lewis acid. The catalytic activity of complex **3a** was variable at different times and temperatures, the best result being obtained at 25 °C for 16 h with a moderate yield of PMMA (run 4). Shorter periods of time and lower temperatures (Table 3, runs 1 and 3) gave lower yields, being significantly much lower when the time was shorter than 5 h. However, periods of time longer than 16 h did not improve the yield, and even lower yields were obtained at temperatures higher than 25 °C, indicating the decomposition of the active species with both time and temperature. The polymers obtained were mainly syndiotactic, with higher syndiotacticity under the conditions corresponding to run 3. When CH_2Cl_2 instead of toluene was employed as the solvent, the polymer obtained was also syndiotactic (over 70%) but in a lower yield and with a higher polydispersity (run 2 vs 3), probably as a consequence of the instability of the Nb−C and Al−C bonds in this solvent. In contrast, the only tantalum aryloxo benzyl derivative isolated, **6a**, showed catalytic activity with both Lewis acids (run 5 and 6), but again with rather poor yields of syndiotactic PMMA.

Activation of **3a** by $Al(C_6F_5)_3$ but not by $B(C_6F_5)_3$ suggests either the formation of an enolate species by benzyl transfer to a MMA·$Al(C_6F_5)_3$ adduct[37,63] or the [4 + 2] addition of MMA to the metal−imido bond, generating a metallacycle.[39] In the case of the neutral complexes **3**–**6** presented in this work, none of them reacted with MMA. Furthermore, we monitored the reaction of MMA·$Al(C_6F_5)_3$ with **3a** in C_6D_6 by NMR spectroscopy, obtaining a mixture of two compounds. Although we have not been able to characterize these compounds, the *t*Bu ^{13}C resonances at δ 71.8 and δ 72.4 confirmed the presence of the imido moiety, in agreement with benzyl transfer to the MMA·$Al(C_6F_5)_3$ adduct. Unfortunately, the ^{19}F NMR spectrum did not allow us to determine the presence of the corresponding enol aluminate anions, due to the number of resonances.

The lesser donor capacity of the NAr imido ligand may explain the lack of activity of **3b**, in agreement with the easy decomposition observed when it was reacted with $E(C_6F_5)_3$. The different activities for MMA polymerization shown by the niobium complex **3a** and the zirconium complex [$ZrCpBz_3$] could be related to the greater kinetic inertness of the Zr−benzyl bond in [$ZrCpBz_3$]. Finally, the activation of **6a** by $B(C_6F_5)_3$ suggests that in this case the tantalum center is responsible for the polymerization activity.

Conclusions

Benzylation with [BzMgCl] of the niobium trichloro imido complexes [$NbCl_3$(NR)$(py)_2$] (R = *t*Bu, Ar; Ar = 2,6-*i*$Pr_2C_6H_3$) previously reported and of the new niobium and tantalum dichloro imido derivatives [MCl_2(NR)(OAr)$(py)_2$] (M = Nb, Ta; R = *t*Bu, Ar) gave the corresponding benzyl complexes [$NbBz_3$(NR)] and [MBz_2(NR)(OAr)(THF)], respectively. The resulting yields depended on the donor capacity of the imido ligand, being moderate to good for the *tert*-butyl but low for the aryl derivatives. The lower σ donor ability of the aryloxo group compared with the benzyl ligand was also responsible for the coordination of one additional THF ligand to give the trigonal-bipyramidal pentacoordinate aryloxo complexes.

One of the benzyl groups of the new isolated imido compounds was abstracted by the Lewis acids $E(C_6F_5)_3$ (E = B, Al) generating the stable zwitterionic complexes [MBz_2(N*t*Bu){η^6-$C_6H_5CH_2E(C_6F_5)_3$}] (M = Nb, Ta; E = B, Al) and [TaBz(N*t*Bu)(OAr){η^6-$C_6H_5CH_2E(C_6F_5)_3$}] (E = B, Al) containing the η^6-coordinated phenyl ring of the benzylborate anion. When these reactions were carried out with imido complexes containing O- and C-donor competing ligands (THF and benzyl, respectively), abstraction of THF by the more oxophilic $Al(C_6F_5)_3$ Lewis acid was the preferred first step of the reaction, whereas the benzyl ligand was first abstracted by the less oxophilic $B(C_6F_5)_3$ reagent. Formation of similar zwitterionic compounds was studied by reactions of the zirconium derivative [$ZrCpBz_3$] with the same Lewis acids $E(C_6F_5)_3$ (E = B,[47] Al).

DFT calculations showed that the cationic fragments $[NbMe_2(N$*t*$Bu)]^+$ and $[ZrCpMe_2]^+$ and the zwitterionic compounds [$NbMe_2$(N*t*Bu){η^6-$C_6H_5CH_2B(C_6F_5)_3$}] (**I**) and [$ZrMe_2Cp$\{η^6-$C_6H_5CH_2B(C_6F_5)_3$\}] (**II**) were isolobal and isoelectronic, respectively. However, both theoretical and NMR data showed a small difference in the coordination of the η^6-benzyl ligand to the niobium atom with respect to the zirconium compound. The antibonding character of the LUMO orbital in complex **I** shows an unfavorable reaction with donor monomers. However, the LUMO orbital in complex **II** has a remarkable bonding character, producing stable interactions with donor ligands. Reactions which imply separation of the ionic pair should be more difficult for complex **I**, due to the higher stabilization energy compared with complex **II**.

Polymerization of methyl methacrylate was achieved with moderate yield for the catalytic system [$NbBz_3$(N*t*Bu)]/$Al(C_6F_5)_3$

(63) Rodríguez-Delgado, A.; Chen, E. Y. X. *Macromolecules* **2005**, *38*, 2587.

and with low yields for the systems [TaBz(N*t*Bu)(OAr)(THF)]/$E(C_6F_5)_3$ (E = B, Al); meanwhile, the zirconium monocyclopentadienyl derivative [ZrCpBz$_3$] only produced traces of PMMA. Two main reasons can be advanced for these results: the reactivity of the metal−imido bond toward unsaturated systems which could interfere with polymerization and the kinetic inertness of the metal−benzyl bond with respect to the usually more active metal−methyl bonds, although we have not been able to isolate this last type of compound. Further studies aimed at a better understanding of the polymerization process are in progress.

Experimental Section

General Considerations. All manipulations were carried out under an argon atmosphere, and solvents were distilled from appropriate drying agents. NMR spectra were recorded at 400.13 (^{1}H), 376.70 (^{19}F), and 100.60 (^{13}C) MHz on a Bruker AV400. Chemical shifts (δ) are given in ppm using C_6D_6 as solvent, unless otherwise stated. ^{1}H and ^{13}C resonances were measured relative to solvent peaks considering TMS at 0 ppm; meanwhile ^{19}F resonances were measured relative to external $CFCl_3$. Assignment of resonances was made from HMQC and HMBC NMR experiments. Elemental analyses were performed on a Perkin-Elmer 240C. The compounds [$TaCl_2$(NAr)(OAr)(py)$_2$],[49] [MCl_3(NR)(py)$_2$] (M = Nb, Ta; R = *t*Bu, Ar),[49,50] $B(C_6F_5)_3$,[64] and $Al(C_6F_5)_3\cdot 0.5$(toluene)[17] were prepared by literature methods.

[$NbCl_2$(N*t*Bu)(OAr)(py)$_2$] (1a; Ar = 2,6-*i*Pr$_2$C$_6$H$_3$). LiOAr·THF (0.60 g, 2.33 mmol) in Et_2O/THF (20 mL/10 mL) was added to a solution of [$NbCl_3$(N*t*Bu)(py)$_2$] (1.00 g, 2.33 mmol) in Et_2O/THF (15:5 mL) at 25 °C. The reaction mixture was stirred for a further 16 h. The resulting yellow solution was separated by filtration, and the volatiles were removed under reduced pressure. The residue was washed with hexane (3 × 15 mL) and then dried to give **1a** as a yellow solid (1.06 g, 80%). ^{1}H NMR: 1.24 (s, 9H, C*Me*$_3$), 1.44 (d, *J* = 6.9 Hz, 12H, *Me*$_2$CH), 4.46 (sept, *J* = 6.9 Hz, 2H, Me$_2$C*H*), 6.45 (m, 4H, *m*-py), 6.75 (m, 2H, *p*-py), 7.05 (m, 1H, *p*-C$_6$*H*$_3$), 7.25 (m, 2H, *m*-C$_6$*H*$_3$), 9.14 (m, 4H, *o*-py). ^{13}C NMR: 24.3 (*Me*$_2$CH), 26.4 (Me$_2$*C*H), 30.3 (C*Me*$_3$) 68.5 (*C*Me$_3$), 121.9 (*p*-C$_6$*H*$_3$), 123.6 (*m*-C$_6$*H*$_3$), 123.7 and 127–6 (*m*-py), 137.3 (*o*-C$_6$*H*$_3$), 137.8 and 137.9 (*p*-py), 151.9 and 152.8 (*o*-py), 162.0 (*i*-C$_6$*H*$_3$). Anal. Calcd for $C_{26}H_{36}Cl_2N_3NbO$ (569.13): C, 54.75; H, 6.36; N, 7.37. Found: C, 55.42; H, 6.20; N, 7.42.

[$NbCl_2$(NAr)(OAr)(py)$_2$] (1b; Ar = 2,6-*i*Pr$_2$C$_6$H$_3$). Following the same methodology described above, complex **1b** was obtained from the reaction of [$NbCl_3$(NAr)(py)$_2$] (1.00 g, 1.88 mmol) in 20 mL of Et_2O/THF (2/1) with LiOAr·THF (0.48 g, 1.88 mmol) in 30 mL of Et_2O/THF (2/1) as a yellow solid (1.01 g, 80%). ^{1}H NMR: 1.25 (m, 24H, *Me*$_2$CH), 4.33 (m, 4H, Me$_2$C*H*), 6.28–6.50 (m, 8H, py), 7.00 (m, 2H, *p*-C$_6$*H*$_3$), 7.05 (m, 4H, *m*-C$_6$*H*$_3$), 8.80 (m, 4H, *o*-C$_6$*H*$_3$), 9.10 (m,2H, *o*-py). ^{13}C NMR: 24.3, 24.8 (*Me*$_2$CH), 26.1, 28.0 (Me$_2$*C*H), 122.4, 122.9, 123.6, 124.3, 125.67, 137.6, 138.1, 147.2, 150.8, 152.6 (*C*$_6$H$_3$ and py), 151.3 (*i*-*C*$_6$H$_3$N), 160.4 (*i*-*C*$_6$H$_3$O). Anal. Calcd for $C_{34}H_{40}Cl_2N_3NbO$ (670.51): C, 60.90; H, 6.01; N, 6.27. Found: C, 60.66; H, 5.85; N, 6.42.

[$TaCl_2$(N*t*Bu)(OAr)(py)$_2$] (2a; Ar = 2,6-*i*Pr$_2$C$_6$H$_3$). Following the same methodology described above, complex **2a** was obtained from the reaction of [$TaCl_3$(N*t*Bu)(py)$_2$] (1.00 g, 1.52 mmol) in 20 mL of Et_2O/THF (2/1) with LiOAr·THF (0.50 g, 1.93 mmol) in 30 mL of Et_2O/THF (2/1) as a yellow solid (1.01 g, 80%). ^{1}H NMR: 1.31 (s, 9H, C*Me*$_3$), 1.44 (d, *J* = 6.9 Hz, 12H, *Me*$_2$CH), 4.41 (sept, *J* = 6.9 Hz, 2H, Me$_2$C*H*), 6.36 and 6.51 (m, 4H, *m*-py), 6.69 and 6.79 (m, 2H, *p*-py), 7.04 (m, 1H, *p*-C$_6$*H*$_3$), 9.11 (m, 4H, *o*-py), 7.28 (m, 2H, *m*-C$_6$*H*$_3$). ^{13}C NMR: 24.5 (*Me*$_2$CH), 26.3 (*Me*$_2$CH), 32.4 (C*Me*$_3$), 68.1 (*C*Me$_3$), 121.7 (*p*-*C*$_6$H$_3$), 123.6 (*m*-*C*$_6$H$_3$), 123.9 and 124.3 (*m*-py), 137.8 and 138.2 (*p*-py), 137.9 (*o*-*C*$_6$H$_3$), 151.2 and 153.3 (*o*-py), 160.0 (*i*-*C*$_6$H$_3$). Anal. Calcd for $C_{26}H_{36}Cl_2N_3OTa$ (658.44): C, 47.43; H, 5.51; N, 6.38. Found: C, 47.20; H, 5.46; N, 6.39.

[$NbBz_3$(N*t*Bu)] (3a). BzMgCl (2 M in THF, 6.99 mmol) was added to a solution of [$NbCl_3$(N*t*Bu)(py)$_2$] (1.00 g, 2.33 mmol) in 20 mL of Et_2O at −78 °C. The resulting yellow mixture was stirred for 16 h at 25 °C, after which the solution was filtered over Celite and the volatiles were removed. The solid product was washed with pentane and dried in vacuo, yield 0.81 g (80%). ^{1}H NMR: 1.35 (s, 9H, C*Me*$_3$), 1.68 (s, 6H, C*H*$_2$Ph), 6.57 (m, 3H, C$_6$*H*$_5$), 6.98 (m, 12H, C$_6$*H*$_5$). ^{13}C NMR: 31.8 (C*Me*$_3$), 53.3 (*C*H$_2$Ph), 125.4 (*p*-*C*$_6$H$_5$), 129.4 (*m*-*C*$_6$H$_5$), 130.1 (*o*-*C*$_6$H$_5$), 136.0 (*i*-*C*$_6$H$_5$), the *i*-*C*Me$_3$ resonance was not observed. Anal. Calcd for $C_{25}H_{30}NNb$ (437.42): C, 68.65; H, 6.91; N, 3.20. Found: C, 68.50; H, 6.87; N, 3.20.

[$NbBz_3$(NAr)] (3b; Ar = 2,6-*i*Pr$_2$C$_6$H$_3$). The same procedure described for **3a** was followed, using [$NbCl_3$(NAr)(py)$_2$] (1.00 g, 1.88 mmol) in 20 mL of Et_2O and BzMgCl (2 M in THF, 5.54 mmol), affording **3b** as a clear yellow solid (0.22 g, 25%). ^{1}H NMR: 1.34 (d, *J* = 6.9 Hz, 12H, *Me*$_2$CH), 1.90 (s, 6H, C*H*$_2$Ph), 4.20 (sept, *J* = 6.9 Hz, 2H, Me$_2$C*H*), 6.62 (m, 3H, C$_6$*H*$_5$), 7.00–7.20 (m, 15H, C$_6$*H*$_3$, C$_6$*H*$_5$). ^{13}C NMR: 24.4 (*Me*$_2$CH), 26.3 (Me$_2$*C*H), 28.4 (*C*H$_2$Ph), 123.0, 124.5, 126.2, 128.5, 128.8, 130.3, (*C*$_6$H$_3$, *C*$_6$H$_5$), 134.9 (*i*-*C*$_6$H$_5$), 144.9 (*i*-*C*$_6$H$_3$). Anal. Calcd for $C_{33}H_{38}NNb$ (541.57): C, 73.19; H, 7.07; N, 3.59. Found: C, 73.25; H, 7.07; N, 2.53.

[$NbBz_2$(N*t*Bu)(OAr)(THF)] (5a; Ar = 2,6-*i*Pr$_2$C$_6$H$_3$). BzMgCl (2 M in THF, 1.40 mmol) was added to a stirred solution of [$NbCl_2$(NAr)(OAr)(py)$_2$] (**1b**; 0.40 g, 0.70 mmol) in 30 mL of Et_2O at −78 °C. The reaction slurry was stirred for 16 h at 25 °C, and then 10 mL of hexane was added. The solution was filtered, and the volatiles were removed at reduced pressure to give **5a** as a yellow solid (0.12 g, 30%). ^{1}H NMR: 0.92 (s, 9H, C*Me*$_3$), 1.31 (d, *J* = 6.9 Hz, 12H, *Me*$_2$CH), 1.36 (m, 4H, *β*-C*H*$_2$, THF), 1.96 (d, *J* = 10.0 Hz, 2H, C*H*$_2$Ph), 2.94 (d, *J* = 10.0, 2H, C*H*$_2$Ph), 3.46 (sept, *J* = 6.9 Hz, 2H, Me$_2$C*H*), 3.70 (m, 4H, α-C*H*$_2$, THF), 6.98–7.20 (m, 13H, C$_6$*H*$_3$ and C$_6$*H*$_5$). ^{13}C NMR: 23.3 (*Me*$_2$CH), 25.3 (*β*-*C*H$_2$, THF), 27.1 (Me$_2$*C*H), 31.3 (C*Me*$_3$), 69.1 (α-*C*H$_2$, THF), 69.2 (*C*H$_2$Ph), 121.3, 123.1, 123.9, 128.9, 129.1, 135.7 (*C*$_6$H$_3$, *C*$_6$H$_5$), 144.0 (*i*-*C*$_6$H$_5$), 162.1 (*i*-*C*$_6$H$_3$); the *i*-*C*Me$_3$ resonance was not observed. Anal. Calcd for $C_{34}H_{48}NNbO_2$ (595.66): C, 68.56; H, 8.12; N, 2.35. Found: C, 68.80; H, 8.20; N, 2.10.

[$TaBz_2$(N*t*Bu)(OAr)(THF)] (6a; Ar = 2,6-*i*Pr$_2$C$_6$H$_3$). The same procedure described above for **5a** was followed using [$TaCl_2$(N*t*Bu)(OAr)(py)$_2$] (0.40 g, 0.60 mmol) and BzMgCl (2 M in THF, 1.21 mmol) to give **6a** as a yellow solid (0.14 g, 35%). ^{1}H NMR: 0.92 (s, 9H, C*Me*$_3$), 1.29 (d, *J* = 6.9 Hz, 12H, *Me*$_2$CH), 1.30 (m, 4H, *β*-C*H*$_2$, THF), 1.90 (d, *J* = 11.4 Hz, 2H, C*H*$_2$Ph), 2.74 (d, *J* = 11.4 Hz, 2H, C*H*$_2$Ph), 3.44 (sept, *J* = 6.9 Hz, 2H, Me$_2$C*H*), 3.66 (m, 4H, α-C*H*$_2$, THF), 6.96–7.12 (m, 13H, C$_6$*H*$_3$ and C$_6$*H*$_5$). ^{13}C NMR: 23.5 (*Me*$_2$CH), 25.4 (*β*-*C*H$_2$, THF), 27.3 (Me$_2$*C*H), 32.6 (C*Me*$_3$), 66.0 (*C*Me$_3$), 69.5 (α-*C*H$_2$, THF), 121.8, 123.2, 123.5, 129.6, 129.9, 135.9 (*C*$_6$H$_3$, *C*$_6$H$_5$), 146.0 (*i*-*C*$_6$H$_5$), 160.6 (*i*-*C*$_6$H$_3$). Anal. Calcd for $C_{34}H_{48}NO_2Ta$ (683.70): C, 59.73; H, 7.08; N, 2.05. Found: C, 60.02; H, 7.42; N, 2.09.

[$TaBz_2$(NAr)(OAr)(THF)] (6b; Ar = 2,6-*i*Pr$_2$C$_6$H$_3$). The same procedure described for **5a** was followed using [$TaCl_2$(NAr)(OAr)(py)$_2$] (0.40 g, 0.52 mmol) and BzMgCl (2 M in THF, 1.04 mmol), giving complex **6b** as an orange solid (0.080 g, 20%). ^{1}H NMR: 1.25 (m, 24H, *Me*$_2$CH), 1.30 (m, 4H, *β*-C*H*$_2$, THF), 2.80 (m, 4H, C*H*$_2$Ph), 3.57 (m, 4H, α-C*H*$_2$, THF), 3.91 (sept, *J* = 6.6 Hz, Me$_2$C*H*), 4.10 (sept, *J* = 6.5 Hz, 2H, Me$_2$C*H*), 6.08–7.18 (m, 16H, C$_6$*H*$_3$ and C$_6$*H*$_5$). We were not able to obtain an adequate elemental analysis for compound **6b**.

[$NbBz_2$(N*t*Bu){η^6-C$_6$H$_5$CH$_2$B(C$_6$F$_5$)$_3$}] (7a-B). In a glovebox, C_6D_6 solutions of the compounds [$NbBz_3$(N*t*Bu)] (**3a**; 0.017 g, 0.034 mmol) and $B(C_6F_5)_3$ (0.015 g, 0.034 mmol) were loaded into

(64) Lancaster, S. In www.syntheticpages.org, 2003, 215.

an NMR tube. The reaction was followed by NMR spectroscopy, resulting in the immediate formation of complex **7a-B** (100%). The solution was layered with hexane to give a microcrystalline yellow solid (0.018 g, 50%). ^{1}H NMR: 0.80 (s, 9H, CMe_3), 1.02 (d, J = 9.0 Hz, 2H, PhCH_2Nb), 1.74 (d, J = 9.0 Hz, 2H, PhCH_2Nb), 3.28 (m, 2H, PhCH_2B), 5.44 (m, 1H, p-$C_6H_5CH_2$B), 5.67 (m, 2H, m-$C_6H_5CH_2$B), 6.34 (m, 4H, o-$C_6H_5CH_2$Nb), 6.49 (m, 2H, o-$C_6H_5CH_2$B), 6.84 (m, 4H, m-$C_6H_5CH_2$Nb), 6.98 (m, 2H, p-$C_6H_5CH_2$Nb). ^{13}C NMR: 30.6 (CMe_3), 36.0 (CH_2B), 45.7 (CH_2Nb), 71.2 (CMe_3) 117.2 (p-$C_6H_5CH_2$B), 122.9 (o-$C_6H_5CH_2$B), 126.2 (m-$C_6H_5CH_2$B), 128.4 ($C_6H_5CH_2$Nb), 129.6 ($C_6H_5CH_2$Nb), 131.2 (i-$C_6H_5CH_2$Nb), 136.5 (C_6F_5), 138.9 (C_6F_5), 148.0 (C_6F_5). ^{19}F NMR: −129.5 (m, 6F, o-C_6F_5), −159.2 (m, 3F, p-C_6F_5), −163.4 (m, 6F, m-C_6F_5). Anal. Calcd for $C_{43}H_{30}BF_{15}NNb$ (949.40): C, 54.40; H, 3.18; N, 1.48. Found: C, 54.13; H, 3.00; N, 1.29.

[NbBz$_2$(N*t*Bu){η^6-C$_6$H$_5$CH$_2$Al(C$_6$F$_5$)$_3$}] (7a-Al). The same procedure described for **7a-B** was followed using [NbBz$_3$(N*t*Bu)] (**3a**; 0.017 g, 0.034 mmol) and Al(C_6F_5)$_3$ (0.017 g, 0.034 mmol), resulting in the immediate formation of complex **7a-Al** (100% by ^{1}H NMR). ^{1}H NMR: 0.71 (s, 9H, CMe_3), 0.84 (d, J = 8.7 Hz, 2H, PhCH_2Nb), 1.83 (d, J = 8.7 Hz, 2H, PhCH_2Nb), 2.76 (m, 2H, PhCH_2Al), 5.21 (m, 1H, p-$C_6H_5CH_2$Al), 5.81 (m, 2H, m-$C_6H_5CH_2$Al), 6.24 (m, 4H, o-$C_6H_5CH_2$Nb), 6.30 (m, 2H, o-$C_6H_5CH_2$Al), 6.81 (m, 4H, m-$C_6H_5CH_2$Nb), 6.99 (m, 2H, p-$C_6H_5CH_2$Nb). ^{13}C NMR: 30.8 (CMe_3), 33.9 (PhCH_2Al), 47.7 (CH_2Nb), 70.9 (CMe_3), 110.4 (p-$C_6H_5CH_2$Al), 120.6 (o-$C_6H_5CH_2$Al), 124.9 (m-$C_6H_5CH_2$Al), 128.5 ($C_6H_5CH_2$Nb), 129.3 ($C_6H_5CH_2$Nb), 129.7 ($C_6H_5CH_2$Nb), 130.9 ($C_6H_5CH_2$Nb), 137.2 (C_6F_5), 141.2 (C_6F_5), 150.4 (C_6F_5), 159.6 (C_6F_5). ^{19}F NMR: −119.9 (m, 6F, o-C_6F_5), −153.5 (m, 3F, p-C_6F_5), −160.8 (m, 6F, m-C_6F_5).

[TaBz$_2$(N*t*Bu){η^6-C$_6$H$_5$CH$_2$Al(C$_6$F$_5$)$_3$}] (8a-Al). The same procedure described for **7a-B** was followed using [TaBz$_3$(N*t*Bu)] (**4a**; 0.016 g, 0.028 mmol) and Al(C_6F_5)$_3$ (0.015 g, 0.028 mmol), resulting in the immediate formation of complex **8a-Al** (100% by ^{1}H NMR). ^{1}H NMR: 0.80 (s, 9H, CMe_3), 0.98 (d, J = 10.5 Hz, 2H, PhCH_2Ta), 1.69 (d, J = 10.5 Hz, 2H, PhCH_2Ta), 2.83 (m, 2H, PhCH_2Al), 5.18 (m, 1H, p-$C_6H_5CH_2$Al), 5.80 (m, 2H, m-$C_6H_5CH_2$Al), 6.29 (m, 2H, o-$C_6H_5CH_2$Al), 6.43 (m, 4H, o-$C_6H_5CH_2$Ta), 6.84 (m, 4H, m-$C_6H_5CH_2$Ta), 7.10 (m, 2H, p-$C_6H_5CH_2$Ta). ^{13}C NMR: 32.0 (CMe_3), 34.0 (PhCH_2Al), 50.7 (PhCH_2Ta), 68.1 (CMe_3), 109.6 (p-$C_6H_5CH_2$Al), 120.4 (o-$C_6H_5CH_2$Al), 125.0 (m-$C_6H_5CH_2$Al), 128.9 ($C_6H_5CH_2$Ta), 129.7 ($C_6H_5CH_2$Ta), 131.7 ($C_6H_5CH_2$Ta), 133.7 ($C_6H_5CH_2$Ta), 139.1 (C_6F_5), 150.1 (C_6F_5), 160.7 (C_6F_5). ^{19}F NMR: −120.9 (m, 6F, o-C_6F_5), −154.3 (m, 3F, p-C_6F_5), −161.7 (m, 6F, m-C_6F_5).

[TaBz(N*t*Bu)(OAr)(THF)][BzB(C$_6$F$_5$)$_3$] (9a; Ar = 2,6-*i*Pr$_2$-C$_6$H$_3$). B(C_6F_5)$_3$ (0.011 g, 0.022 mmol) was added to a solution of compound **6a** (0.015 g, 0.022 mmol) in C_6D_6. The precipitation of an oil was immediately observed. This was then separated from the C_6D_6 solution and dissolved in C_6D_5Br. The NMR spectra of the solution at 25 °C showed the formation of complex **9a**. ^{1}H NMR (C_6D_5Br): 1.08 (s, 9H, CMe_3), 1.10 (d, J = 6.7 Hz, 12H, Me_2CH), 1.33 (m, 4H, β-CH_2, THF), 1.50 (m, 2H, PhCH_2Ta), 3.27 (m, 2H, PhCH_2-B), 3.43 (m, 2H, Me$_2$CH), 3.83 (m, 4H, α-CH_2, THF), 6.70–7.10 (m, 13H, C_6H_3 and C_6H_5). ^{13}C NMR (C_6D_5Br): 23.4 (Me_2CH), 25.6 (Me$_2$CH), 26.4 (β-CH_2, THF), 32.0 (PhCH_2B), 33.6 (CMe_3), 65.0 (α-CH_2, THF), 68.7 (CMe_3), 74.8 (PhCH_2−Ta), 123.2, 124.6, 125.3, 127.5, 129.4, 132.5, 149.3, (C_6H_3, C_6H_5), 137.6 (i-C_6H_5), 154.7 (i-C_6H_3), 126.7 (C_6F_5), 129.6 (C_6F_5), 131.5 (C_6F_5). ^{19}F NMR (C_6D_5Br): −128.9 (m, 6F, o-C_6F_5), −162.3 (m, 3F, p-C_6F_5), −165.2 (m, 6F, m-C_6F_5).

[TaBz$_2$(N*t*Bu)(OAr)] (10a; Ar = 2,6-*i*Pr$_2$C$_6$H$_3$). Al(C_6F_5)$_3$ (0.012 g, 0.022 mmol) was added to a solution of compound **6a** (0.015 g, 0.022 mmol) in C_6D_6. The reaction was monitored by NMR spectroscopy to determine the formation of complex **10a** and the adduct THF·Al(C_6F_5)$_3$. ^{1}H NMR: 0.98 (m, 4H, β-CH_2, THF), 1.12 (s, 9H, CMe_3), 1.20 (d, J = 6.9 Hz, 12H, Me_2CH), 1.87 (d, J = 11.4 Hz, 2H, PhCH_2), 2.61 (d, J = 11.4 Hz, 2H, PhCH_2), 3.40 (m, 6H, Me$_2$CH and α-CH_2 THF), 6.90–7.15 (m, 18H, C_6H_3 and C_6H_5). ^{13}C NMR: 23.5 (Me_2CH), 24.9 (Me$_2$CH), 27.1 (β-CH_2, THF), 33.8 (CMe_3), 65.1 (α-CH_2, THF), 67.5 (CMe_3), 73.8 (CH_2Ph), 122.9, 123.3, 125.3, 125.6, 128.5, 129.3, 129.5, 129.7, 136.9, 147.1 (C_6H_3, C_6H_5), 139.8 (i-C_6H_5), 158.4 (i-C_6H_3), 137.1 (C_6F_5), 142.0 (C_6F_5), 150.0 (C_6F_5).

[TaBz(N*t*Bu)(OAr){η^6-C$_6$H$_5$CH$_2$E(C$_6$F$_5$)$_3$}] (E = B (11a-B), Al (11a-Al); Ar = 2,6-*i*Pr$_2$C$_6$H$_3$). In a glovebox, C_6D_6 solutions of compounds **6a** (0.015 g, 0.022 mmol) and E(C_6F_5)$_3$ (E = B, Al; 0.044 mmol), were added to a Teflon-valved NMR tube. The reaction was monitored by NMR spectroscopy to determine the formation of compounds **11a-E** and the adducts THF·E(C_6F_5)$_3$. Complex **11a-B**: ^{1}H NMR 1.10 (m, 4H, β-CH_2, THF), 1.18 (m, 21H, Me_2CH and CMe_3), 2.33 (d, J = 8.7 Hz, 1H, PhCH_2Ta), 3.24 (m, 6H, α-CH_2 THF and PhCH_2B), 3.46 (m, 2H, Me$_2$CH), 3.62 (d, J = 8.7 Hz, 1H, PhCH_2Ta), 6.20–7.20 (m, 13H, C_6H_3 and C_6H_5); ^{13}C NMR 22.9 (Me_2CH), 23.1 (Me$_2$CH), 27.3 (β-CH_2, THF), 29.0 (PhCH_2B), 32.9 (CMe_3), 59.0 (α-CH_2, THF), 76.0 (PhCH_2Ta), 123.3, 123.5, 124.8, 125.6, 126.3, 129.3, 130.5, 131.5, 136.4, 146.3 (C_6H_3, C_6H_5), 141.6 (i-C_6H_5), 152.0 (i-C_6H_5), 137.3 (C_6F_5), 144.8 (C_6F_5), 148.5 (C_6F_5), the i-CMe_3 resonance was not observed; ^{19}F NMR −130.2 (m, 6F, o-C_6F_5), −154.2 (m, 3F, p-C_6F_5), −161.4 (m, 6F, m-C_6F_5). Complex **11a-Al**: ^{1}H NMR 0.98 (m, 4H, β-CH_2, THF), 1.16 (m, 12H, Me_2CH), 1.19 (s, 9H, CMe_3), 2.34 (d, J = 8.7 Hz, 1H, PhCH_2Ta), 3.20 (m, 2H, PhCH_2Al), 3.43 (m, 6H, Me$_2$CH and α-CH_2 THF), 3.62 (d, J = 8.7 Hz, 1H, PhCH_2Ta), 6.10–7.20 (m, 18H, C_6H_3, C_6H_5). ^{13}C NMR: 23.4 (Me_2CH), 24.8 (Me$_2$CH), 27.0 (β-CH_2, THF), 29.0 (PhCH_2Al), 33.0 (CMe_3), 65.0 (α-CH_2, THF), 67.2 (CMe_3), 74.0 (PhCH_2Ta), 122.8, 123.2, 125.2, 125.5, 128.4 129.1, 129.4, 129.6, 131.2, 136.2, 136.8, 137.7, 142.4, 146.9 (C_6H_3, C_6H_5), 139.6 (i-C_6H_5), 158.3 (i-C_6H_3), 137.2 (C_6F_5), 142.0 (C_6F_5), 150.5 (C_6F_5); ^{19}F NMR −123.3 (m, 6F, o-C_6F_5), −151.5 (m, 3F, p-C_6F_5), −161.1 (m, 6F, m-C_6F_5).

[Zr(η^5-C$_5$H$_5$)Bz$_2${η^6-C$_6$H$_5$CH$_2$Al(C$_6$F$_5$)$_3$}] (12-Al). In a glovebox, C_6D_6 solutions of the compounds [ZrCpBz$_3$] (0.018 g, 0.042 mmol) and Al(C_6F_5)$_3$ (0.042 mmol) were mixed in a Teflon-valved NMR tube. The reaction was followed by NMR spectroscopy, and the formation of compound **12-Al** was observed (100% by ^{1}H NMR). ^{1}H NMR: 1.48 (d, J = 11 Hz, 2H, PhCH_2Zr), 1.59 (d, J = 11 Hz, 2H, PhCH_2Zr), 2.64 (b.s., 2H, PhCH_2Al), 5.21 (s, 5H, C_5H_5), 5.58 (b.s., 1H, p-$C_6H_5CH_2$Al), 5.80 (br s, 2H, m-$C_6H_5CH_2$Al), 6.16 (br s, 2H, o-$C_6H_5CH_2$Al), 6.80–7.20 (m, 15H, $C_6H_5CH_2$ and C_6H_5Me). ^{19}F NMR: −119.9 (m, 6F, o-C_6F_5), −154.5 (m, 3F, p-C_6F_5), −161.4 (m, 6F, m-C_6F_5).

X-ray Structure Determination of 3a ($C_{25}H_{30}NNb$, M_r = 437.41). Single crystals of **3a** suitable for the X-ray diffraction study were grown from hexane. A yellow crystal was selected, covered with perfluorinated ether and mounted on a Bruker-Nonius Kappa CCD single-crystal diffractometer equipped with graphite-monochromated Mo Kα radiation (λ = 0.710 73 Å). Data collection was performed at 200(2) K: crystal dimensions 0.22 × 0.18 × 0.16 mm, trigonal crystal system, space group $P3_1c$, a = 11.2683(13) Å, c = 10.2514(11) Å, V = 1127.3(2) Å^3, Z = 2, ρ_{calcd} = 1.289 g cm^{-3}, F(000) = 456, 9387/1724 collected/unique reflections (R(int) = 0.0868), θ range 3.62−27.49°. Multiscan[65] absorption correction procedures were applied to the data (μ = 0.542 mm^{-1}, minimum/maximum transmission 0.749/0.918). The structure was solved, using the WINGX package,[66] by direct methods (SHELXS-97) and refined by using full-matrix least squares against F^2 (SHELXL-97).[67] All non-hydrogen atoms were anisotropically refined. Hydrogen atoms were geometrically placed and left riding on their parent atoms. Full-matrix least-squares refinements were carried

(65) Blessing, R. H. *Acta Crystallogr., Sect. A* **1995**, *51*, 33.
(66) Farrugia, L. J. *J. Appl. Crystallogr.* **1999**, *32*, 837.
(67) Sheldrick, G. M. *SHELXL-97*; University of Gottingen, Gottingen, Germany, 1998.

out by minimizing $\sum w(F_o^2 - F_c^2)^2$ with the SHELXL-97 weighting scheme and stopped at shift/error <0.001. The final cycle of full-matrix least-squares refinement based on 1724 reflections and 82 parameters converged to final values of $R1(F^2 > 2\sigma(F^2)) = 0.0327$, $wR2(F^2 > 2\sigma(F^2)) = 0.0557$, $R1(F^2) = 0.0497$, $wR2(F^2) = 0.593$). Final difference Fourier maps showed no peaks higher than 0.190 e Å^{-3} or deeper than −0.284 e Å^{-3}. CCDC-655227 (**3a**) contains the supplementary crystallographic data for this paper. This data can be obtained free of charge from The Cambridge Crystallographic Data Centre via www.ccdc.cam.ac.uk/data_request/cif.

Computational Methods. All energies and geometries were calculated using the B3P86 hybrid DFT method as implemented in Gaussian03.[68] This method consists of two different functionals: the Becke-3 parameter hybrid exchange functional[69] and the Perdew 86 correlation functional.[70] Both potentials use nonlocal exchange-correlation corrections to the density. The current method has shown to reproduce experimental geometries in which there are weak coordinative bonds similar to those in the organometallic compounds studied here.[71] The electronic configurations of the atoms were described by a double-ζ basis set on all atoms. The basis set was augmented with a double-polarization function for all atoms but the metal atom, in which a single $(n + 1)$p polarization function was added.[72,73] The core electrons were treated by the relativistic LANL2 pseudopotential.[74] The most stable arene conformers were previously searched by scanning N−Nb−X1−C and X2−Zr−X1−C dihedral angles for complexes **I** and **II**, respectively (see Figure 2 for nomenclature). The main difference between the complexes is the relative position of the $CH_2B(C_6F_5)_3$ moiety with respect to the metal fragment. After that, all conformers were optimized without any constraint. Differences less than 2.0 kcal mol^{-1} have been found for the different conformers, indicating an easy rotation of the arene fragment. In the present paper, we only show the most stable conformers for both complexes. The atomic orbital contributions and overlap populations were calculated with AOMix software.[75,76] The analysis of the MO composition in terms of occupied and unoccupied fragment molecular orbitals (OFO and UFO, respectively) and construction of molecular orbital interaction diagrams were performed with the AOMix-CDA package.[77]

Polymerization of MMA. The catalyst (4.8×10^{-5} mol) and activator $E(C_6F_5)_3$ (E = B, Al; 9.6×10^{-5} mol) were handled in the glovebox and introduced into an ampule. The temperature desired was adjusted, and a solution of MMA (9.35 mmol) in 3 mL of toluene was added using Schlenk−vacuum-line techniques. The polymerization was terminated by adding MeOH/HCl. The isolated polymer was washed first with MeOH/HCl and then with MeOH/water and dried overnight in vacuo at 60 °C. A ^{1}H NMR ($CDCl_3$) study of the polymer was carried out to determine its tacticity. Melting temperatures of polymers were measured by differential scanning calorimetry (DSC, Perkin-Elmer DSC6). Gel permeation chromatography (GPC) analyses of polymer samples were carried out in THF at 25 °C (Waters GPCV-2000).

Acknowledgment. We gratefully acknowledge Ministerio de Educación y Ciencia (project MAT2007-60997 and MAT2006-0400) and DGUI-Comunidad de Madrid (programme S-0505/PPQ-0328 COMAL-CM) (Spain) for financial support. J.R. thanks CSIC for financial support through an I3P postdoctoral tenure track and R. A. A.-M. MECD for Fellowship. Authors are grateful to Centro Técnico de Informática (CTI-CSIC) for allocation of CPU time on their multiprocessor ORIGIN workstations.

Supporting Information Available: A CIF file giving crystal data for **3b** and figures giving relevant frontier molecular orbitals for the fragment **I.a**, significant molecular orbitals for complexes **I** and **II**, and selected NMR spectra. This material is available free of charge via the Internet at http://pubs.acs.org.

OM701068H

(68) Frisch, M. J.; Trucks, G. W.; Schlegel, H. B.; Scuseria, G. E.; Robb, M. A.; Cheeseman, J. R.; Montgomery, J., J. A.; Vreven, T.; Kudin, K. N.; Burant, J. C.; Millam, J. M.; Iyengar, S. S.; Tomasi, J.; Barone, V.; Mennucci, B.; Cossi, M.; Scalmani, G.; Rega, N.; Petersson, G. A.; Nakatsuji, H.; Hada, M.; Ehara, M.; Toyota, K.; Fukuda, R.; Hasegawa, J.; Ishida, M.; Nakajima, T.; Honda, Y.; Kitao, O.; Nakai, H.; Klene, M.; Li, X.; Knox, J. E.; Hratchian, H. P.; Cross, J. B.; Bakken, V.; Adamo, C.; Jaramillo, J.; Gomperts, R.; Stratmann, R. E.; Yazyev, O.; Austin, A. J.; Cammi, R.; Pomelli, C.; Ochterski, J. W.; Ayala, P. Y.; Morokuma, K.; Voth, G. A.; Salvador, P.; Dannenberg, J. J.; Zakrzewski, V. G.; Dapprich, S.; Daniels, A. D.; Strain, M. C.; Farkas, O.; Malick, D. K.; Rabuck, A. D.; Raghavachari, K.; Foresman, J. B.; Ortiz, J. V.; Cui, Q.; Baboul, A. G.; Clifford, S.; Cioslowski, J.; Stefanov, B. B.; Liu, G.; Liashenko, A.; Piskorz, P.; Komaromi, I.; Martin, R. L.; Fox, D. J.; Keith, T.; Al-Laham, M. A.; Peng, C. Y.; Nanayakkara, A.; Challacombe, M.; Gill, P. M. W.; Johnson, B.; Chen, W.; Wong, M. W.; Gonzalez, C.; Pople, J. A. Gaussian 03, Revision B.05; Gaussian, Inc., Wallingford, CT, 2004.

(69) Becke, A. D. *J. Chem. Phys.* **1992**, *96*, 2155.

(70) Perdew, J. P. *Phys. Rev. B* **1986**, *33*, 8822.

(71) Mihaylov, T.; Trendafilova, N.; Kostova, I.; Georgieva, I.; Bauer, G. *Chem. Phys.* **2006**, *327*, 209.

(72) Sosa, C.; Andzelm, J.; Elkin, B. C.; Wimmer, E.; Dobbs, K. D.; Dixon, D. A. *J. Phys. Chem.* **1992**, *96*, 6630.

(73) Godbout, N.; Salahub, D. R.; Andzelm, J.; Wimmer, E. *Can. J. Chem.* **1992**, *70*, 560.

(74) Hay, P. J.; Wadt, W. R. *J. Chem. Phys.* **1985**, *82*, 270.

(75) Gorelsky, S. I.; Lever, A. B. P. *J. Organomet. Chem.* **2001**, *635*, 187.

(76) Gorelsky, S. I. AOMix: Program for Molecular Orbital Analysis; York University, Toronto, Canada, 1997.

(77) Solomon, E. I.; Gorelsky, S. I.; Dey, A. *J. Comput. Chem.* **2006**, *27*, 1415.